Optics Communications 420 (2018) 122–126

Contents lists available at ScienceDirect

Optics Communications

journal homepage: www.elsevier.com/locate/optcom

Reducing machine-ruling grating wavefront value by compensating grating substrate surface error in real time

Chao Yang [a,*], Yuanhe Li [a], Changxi Xue [a], Xiaotian Li [b,*], Haili Yu [b]

[a] Changchun University of Science and Technology, China
[b] Grating Technology Laboratory, Changchun Institute of Optics and Fine Mechanics and Physics, Chinese Academy of Sciences, China

ARTICLE INFO

OCIS:
050.1950
120.5050
220.4830
120.0120

Keywords:
Diffraction grating
Phase measurement
System design
Grating wavefront

ABSTRACT

To improve the grating wavefront quality especially the grating size, which is more than 1 m, we provide a method based on conical diffraction theory and grating groove active control technology to correct the grating substrate surface error. We apply the grating groove active control technology to carry out an echelle grating ruling experiment whose line density is 79 lines/mm in 36th order. Compared with the grating substrate surface error, the grating wavefront value reduces from 0.105 λ to 0.056λ i.e., decreases by 47%. The experimental result proves that the grating substrate surface error compensation method can be used to improve the grating wavefront quality effectively.

1. Introduction

Plane diffraction gratings especially the echelle grating in meters, which is ruled on the surface of aluminum or other materials such as gold and used in the UV to infrared band, are very popular in military, astronomy, defense, and civilian applications because of their excellent optical functions [1,2]. The main production methods for the echelle grating are mechanical ruling and wet etching techniques [3]. Among them, the wet etching method, which is limited by the processing technology, is generally limited to the manufacture of small-scale echelle grating. Moreover, the etching object of the method is an anisotropic crystal material, for which it is difficult to arbitrarily change the groove shapes according to requirements. Thus, the effect of the manufactured grating is difficult to reach the ideal design value of grating diffraction efficiency. Therefore, the echelle grating is still produced by mechanical ruling currently.

As the quality of diffraction wavefront has a large impact on grating optical properties, foreign researchers paid much attention to it. For mechanically ruled grating, the diffracted wavefront error in fact comprises the substrate surface error and the ruling error [4,5]. Previous investigations have made considerable research on how the grating ruling error can be reduced. The American MIT-A grating ruling machine [6,7] corrected the link mode of the ruling tool system and the ball bearing structure; in this case, the torque can be absorbed by the ball bearing, reducing the grating ruling error, which is generated by the instantaneous torque. Harrison also made corrections to the grating ruling error of the United States MIT-C grating ruling machine, by increasing the thickness of the guide rail from 50 to 100 mm and reducing the grating curve line error, which is generated by the lateral force of the rail during the grating ruling process. Furthermore, the grating ruling machine has a double table carriage to correct the yaw error [8]. In our previous work, it was demonstrated that if we correct the yaw error by using the double piezoelectric ceramics (PZT) to control the inner carriage; the yaw error could be reduced from 0.2″ to 0.027″, i.e., reduced about 86.5% [9]. Furthermore, we have previously provided a method to monitor the grating ruling quality directly in real time, and thus, we can improve the grating ruling quality effectively [10]. Changes in the grating ruling environment will have an impact on the grating ruling error; therefore, the MIT-C grating ruling machine controlled the temperature in the ruling zone to be <0.005 °C and that in the vicinity of the laser to be <0.01 °C by air cooling [11]. The key components were made of Invar material to reduce the effects of thermal expansion. Japan's Hitachi-4 grating ruling machine was also placed under vibration isolation condition to maintain a temperature fluctuation within 0.01 °C [12]. CIOMP-2 grating ruling machine of China was placed in a double enclosure using four air springs to support the grating ruling machine body to achieve the vibration isolation effect, and the thermostat controlled the temperature fluctuation within

* Corresponding authors.
E-mail addresses: yangchaoby@sina.com (C. Yang), lixt_1981@163.com (X.T. Li).

https://doi.org/10.1016/j.optcom.2018.03.024
Received 6 November 2017; Received in revised form 3 March 2018; Accepted 8 March 2018
Available online 1 April 2018

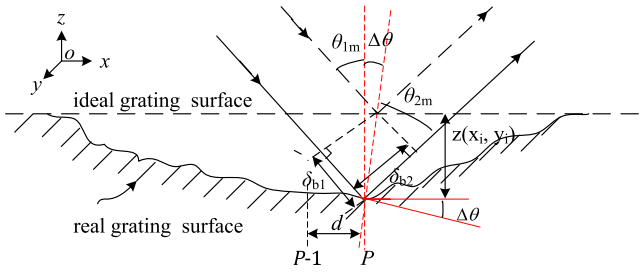

Fig. 1. Optical path difference caused by the grating substrate surface error.

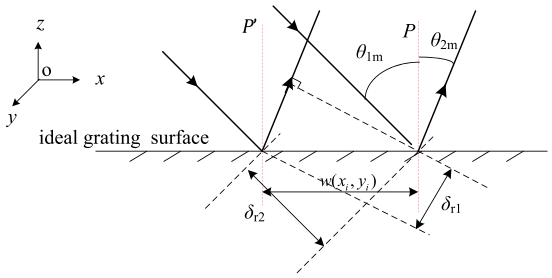

Fig. 2. Optical path difference caused by the ruling system error.

±0.05 °C [13,14]. Recently, the Changchun Institute of Optics and Fine Mechanics and Physics has researched a grating ruling machine CIOMP-6 with a maximum ruling size of 400 mm × 500 mm, whose thermostat controlled the temperature fluctuation within ± 0.007 °C.

The quality of the grating wavefront was also improved by reducing the grating substrate surface error. However, it is difficult to guarantee whether the grating substrate surface is good enough and the coating is completely uniform, especially for gratings at the meter level. The wavefront error generated by the substrate surface of grating will be added directly to the ruling grating as an initial error, which has a greater impact on the grating wavefront value. To solve these problems, this paper proposes a method for compensating the grating substrate surface error, and the paper is organized as follows. In Section 2, we establish a mathematical model for compensating the grating substrate surface error on the basis of the conical diffraction theory [15,16]. In Section 3, we introduce a method, namely the grating groove active control technology, to correct the grating substrate surface error in real time . In Section 4, we apply the above technique to the actual ruling experiment, and the relative result is provided. The conclusion is given in Section 5.

2. Mathematical model for compensating the grating surface error in real time

In Fig. 1, abscissa x represents the length of the grating and ordinate y represents the direction of the grating groove. $\Delta\theta$ is the error angle of the grating substrate surface of the Pth groove [17]. Considering a grating without groove errors but with substrate surface errors, and assuming that a monochromatic parallel light is incident on the planar reflection grating surface, the pattern of incidence is cone diffraction. $\theta_{1m}+\Delta\theta$ and θ_2 represent the incident angle and the diffraction angle, respectively. The angle between the incident ray and the principal section the grating is φ_1, and the angle between the diffraction ray and the main section of grating is φ_2. d is the grating constant. For the convenience of discussion, we assume that the light is incident along the principal section of grating, when $\varphi 1$ and $\varphi 2$ are equal to zero. The grating groove direction is along the y-axis, which is perpendicular to the plane of the figure. When a depth error exists in the form $z(x_i, y_i)$ at the actual position point P, the optical path difference of the incident light at this point δ_{b1} can be given as follows:

$$\delta_{b1} = \frac{z(x_i, y_i)\cos(\theta_{1m} \pm \Delta\theta)}{cos\Delta\theta} = z(x_i, y_i)(\cos\theta_{1m} \mp \Delta\theta \sin\theta_{1m}) \tag{1}$$

The optical path difference of the diffracted light at this point δ_{b2} can be given as follows:

$$\delta_{b2} = \frac{z(x_i, y_i)\cos\theta_{2m}}{cos\Delta\theta} = z(x_i, y_i)\cos\theta_{2m} \tag{2}$$

The optical path difference caused by the substrate surface error at point P is given as follows:

$$\delta_{blank} = \delta_{b1} + \delta_{b2} = z(x_i, y_i)(\cos\theta_{1m} + \cos\theta_{2m} \mp \Delta\theta \sin\theta_{1m}) \tag{3}$$

For different positions of the grating groove, the depth error $z(x_i, y_i)$ is different,

$$z(x_i, y_i) = \begin{bmatrix} x_1 & y_1 \\ x_2 & y_2 \\ \vdots & \vdots \\ x_i & y_i \end{bmatrix} \tag{4}$$

We intend to improve the grating wavefront quality by compensating the grating substrate surface error with the grating groove errors. When the grating substrate surface error does not exist, only the grating groove error is present; as shown in Fig. 2, P is the actual position of the grating groove and P' is the ideal position. If the Pth groove position error exists, the difference between the actual groove position and the ideal groove position is $w(x_i, y_i)$. The optical path difference at this time of the incident and diffracted light generated at point P is given as follows:

$$\delta_{ruling} = \delta_{r1} + \delta_{r2} = w(x_i, y_i)(\sin\theta_{1m} + \sin\theta_{2m}) \tag{5}$$

When φ_1 and φ_2 are not equal to zero, the optical path difference caused by the grating substrate surface error is the same as given in Eq. (3). Here, the optical path difference caused by the groove error is given as follows:

$$\delta_{ruling} = w(x_i, y_i)(\sin\theta_{1m}\cos\varphi_1 + \sin\theta_{2m}\cos\varphi_2) \tag{6}$$

Considering that m is the grating diffraction order and λ is the wavelength, the grating equation can be given as follows:

$$d(\sin\theta_{1m}\cos\varphi_1 + \sin\theta_{2m}\cos\varphi_2) = m\lambda \tag{7}$$

The optical path difference caused by the grating groove error can be calculated from Eqs. (6) and (7), as shown in Eq. (8):

$$\delta_{ruling} = w(x_i, y_i)\frac{m\lambda}{d} \tag{8}$$

Ideally, the grating wavefront error is equal to zero, which means that the sum of the grating substrate surface error and the ruling error is equal to zero.

$$\delta_{blank} + \delta_{ruling} = 0 \tag{9}$$

The grating substrate surface error can be compensated by controlling the ruling position of the diamond tool by the grating groove active control technology. Substituting Eqs. (3) and (8) into Eq. (9), we have the following:

$$w(x_i, y_i) = -z(x_i, y_i)(\cos\theta_{1m} + \cos\theta_{2m} \mp \Delta\theta \sin\theta_{1m})\frac{d}{m\lambda} \tag{10}$$

In general, when a ZYGO interferometer is used to test the grating diffracted wavefront, the monochromatic light incident angle is equal to the absolute value of the diffraction angle. Furthermore,

$$\sin\Delta\theta = \frac{z(x_i, y_i)}{d} \ll \theta_{1m} \tag{11}$$

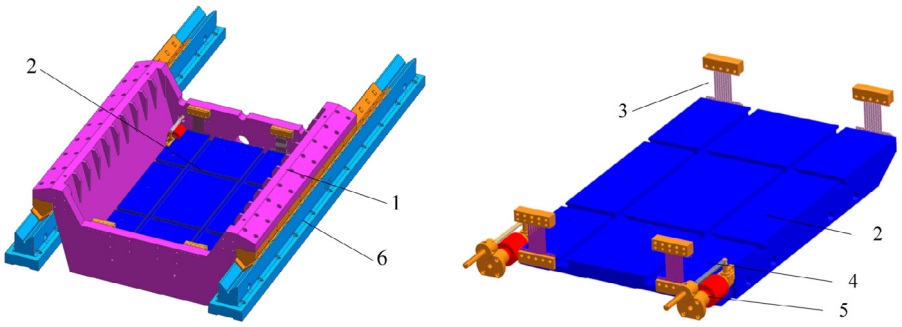

Fig. 3. Working carriage of the grating ruling machine; 1, outer carriage; 2, inner carriage; 3, flexible steel; 4, tension spring; 5, PZT; 6, rails.

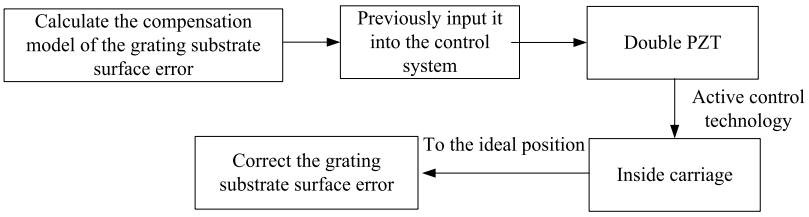

Fig. 4. Solving the compensation model of the grating substrate surface error.

Therefore, we can ignore the effect of $\Delta\theta$, and the compensation model of the grating substrate surface error is obtained as follows:

$$w(x_i, y_i) = -2z(x_i, y_i)\frac{d}{m\lambda}\cos\theta_{1m} \tag{12}$$

3. Active control of the grating surface in real time

In order to correct the grating substrate surface error, we use the grating groove active control technology on the working carriage.

3.1. Working carriage structure

The working carriage structure is shown in Fig. 3. It comprises an outer carriage (1) and an inner carriage (2). The inner carriage hangs in the outer carriage by four parallel flexible steels (3). The four flexible steels are perpendicular to the axis of the moving direction and symmetrically installed on both sides of the working carriage, to ensure the center of gravity balance and provide the displacement and yaw freedom of the working carriage. The double PZT (5) drives the inner carriage to the ideal position, and the tension spring (4) provides an initial closure force of the inner and outer carriage.

3.2. Using grating groove active control technology to correct the grating substrate surface error

The grating groove active control technology uses a double PZT to drive the inner carriage to the ideal position, in order to achieve the grating substrate surface error correction. In the grating substrate surface error compensation process, we measure the grating substrate surface error using the Zygo interferometer (GPITM XP) and first convert it to a xyz three-dimensional coordinate form. Then, we obtain the grating substrate surface error compensation model from Eq. (12); furthermore, the error is inputted into the pre-set control system. During the micro-positioning operation process [18], the diamond tool position is kept unchanged; at this time, the inner carriage is driven to the ideal position by the double PZT, and the drive amount is according to the error compensation model. From the diamond tool falling to the grating surface, the correction of the grating substrate surface error is performed simultaneously with grating ruling. The flow chart for the correction of the grating substrate surface shape error is shown in Fig. 4.

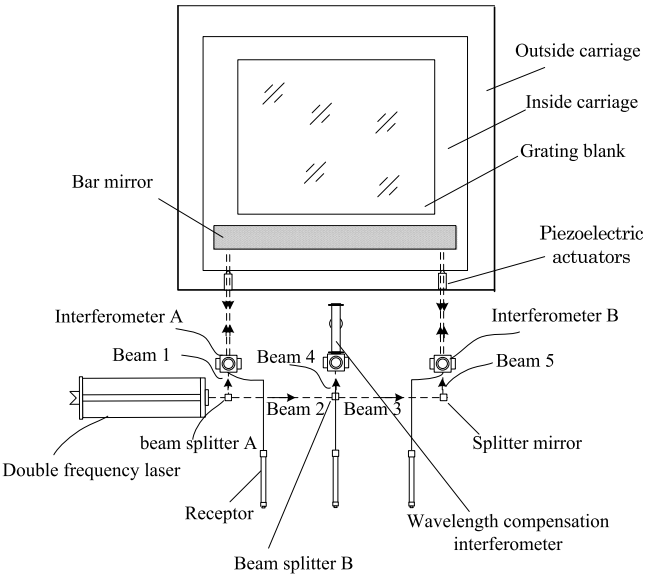

Fig. 5. Optical path of the indexing system.

3.3. Measuring system

In a previous study, it was found that the error of grating indexing system is more obvious than that of grating ruling system on the grating wavefront quality [19]. Therefore, we design a light testing structure to obtain the indexing system error, which is shown in Fig. 5. A laser beam with $\lambda = 632.8$ nm is split into two parts by a beam splitter A. Beam 1 incident on interferometer A, and beam 2 incident on beam splitter B. Beam 4 incident on the wavelength compensation interferometer to compensate errors, which are produced by the change in refractive index of air, and beam 5 incident on interferometer B. When the dividing motor runs a groove space, the working carriage produces an error; we then adjust the length of the PZT to make the inner carriage to the ideal position in order to correct the indexing system error. A testing mirror is placed on the inner carriage as the measuring mirror of the

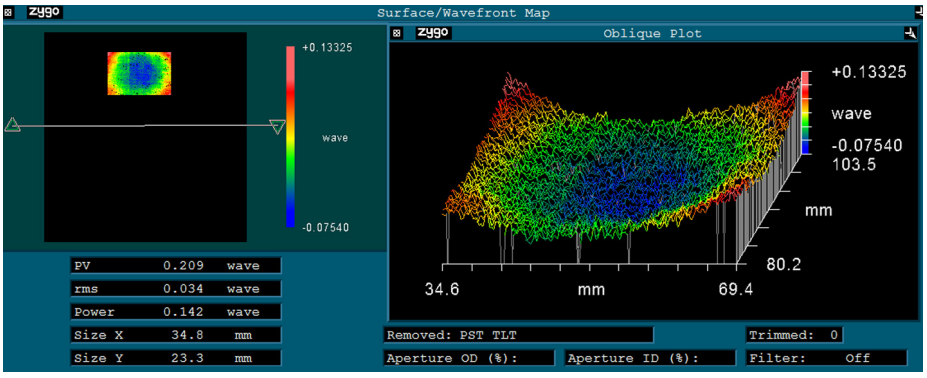

Fig. 6. The wavefront of the grating substrate surface.

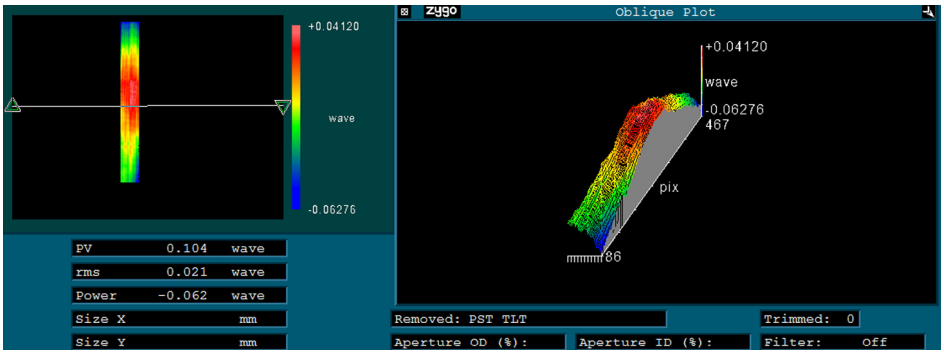

Fig. 7. The 36-order wavefront diagram of the echelle grating.

interferometer light path. Because the testing mirror has a surface error, which affects the wavefront of the grating directly, we must exclude it in the final result.

4. Experiment

In order to verify the feasibility of the grating substrate surface error compensation theory, we have ruled a grating whose size is 35 mm × 90 mm , groove density is 79 lines/mm, and the diffraction order is 36. The grating substrate surface error is directly measured to be 209λ using the Zygo interferometer, as shown in Fig. 6.

We have ruled an echelle grating by the grating substrate surface error compensation method and the grating groove active control technology. The grating diffraction wavefront order is 36; therefore, we carry out the error compensation experiment in the 36th order and obtain a 36th-order diffracted wavefront Δ_{pre} of 0.104λ, which is shown in Fig. 7. The grating ruling machine is a two-dimensional working carriage, and the diamond tool is fixed on a saddle-shaped slider, which reciprocates along the testing mirror. In this case, the surface error of the testing mirror makes the grating grooves to have a bending error, which must be removed. First, we obtain the surface error of the testing mirror using the Zygo interferometer and extract the curve, which is shown in the center of the interferometer spot. It is then interpolated into an array, which is equal to the number of grating wavefront columns $W = [w_1, w_2 \ldots w_n]T$. According to Eq. (8), the surface error of the testing mirror affects the ruled grating wavefront error in the form of ruling errors. Finally, according to Eq. (13), a grating wavefront of 0.056λ is obtained, as shown in Fig. 8, and this is the final compensation result of the grating substrate surface error. (Because the unit of the measurement result of the Zygo interferometer is λ, the λ in the formula must be eliminated.)

$$\Delta = \begin{bmatrix} \delta_{11} & \delta_{12} & \cdots & \delta_{1m} \\ \delta_{21} & \delta_{22} & \cdots & \delta_{2m} \\ & & \vdots & \\ \delta_{n1} & \delta_{n2} & \cdots & \delta_{nm} \end{bmatrix} - \frac{m}{d} \begin{bmatrix} w_1 & w_1 & \cdots & w_1 \\ w_2 & w_2 & \cdots & w_2 \\ & & \vdots & \\ w_n & w_n & \cdots & w_n \end{bmatrix} \tag{13}$$

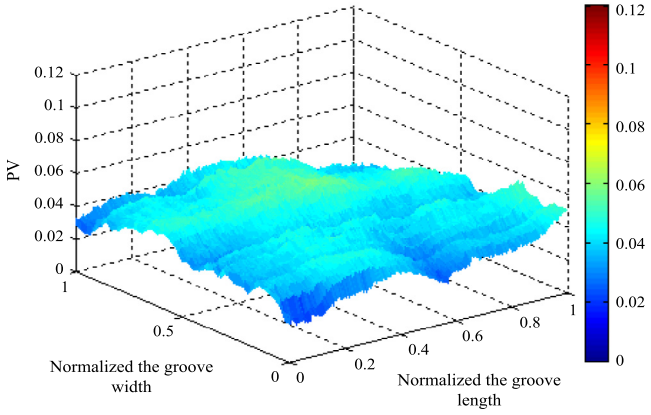

Fig. 8. The 36th-order wavefront diagram after the removal of the surface error of testing mirror.

We need to convert the grating substrate surface error, which is shown in Fig. 6, to its wavefront value at +36th order. Comparing the grating substrate surface error in Fig .6 with the result in Fig. 8, which is in accordance with Eq. (3), and ignoring the effect of $\Delta\theta$ on the wavefront of the grating substrate surface error, we can obtain the grating substrate surface error as follows:

$$\delta_{blank} = \delta_{b1} + \delta_{b2} = 2z(x_i, y_i)\cos\theta_{1m} \tag{14}$$

Then,

$$\delta_{blank} = \delta_{b1} + \delta_{b2} = 2z(x_i, y_i)\sqrt{1 - \frac{m^2\lambda^2}{4d^2}} \tag{15}$$

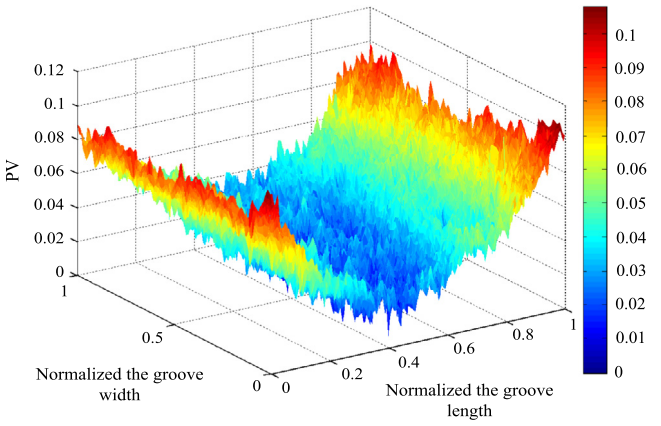

Fig. 9. The 36th-order wavefront diagram of the grating substrate surface.

According to Eq. (15), we obtain the grating substrate surface error at +36th order as shown in Fig. 9, whose wavefront value is 0.105λ.

By comparing Fig. 8 with Fig. 9, the grating substrate surface error is changed from concave to plane, and the grating wavefront value reduces from 0.105λ to 0.056λ, i.e., by 47%. Therefore, the grating substrate surface error is improved significantly.

5. Conclusion

In this paper, we introduce a method for compensating the grating wavefront. We establish a mathematical model according to the conical diffraction theory, and input it to the ruling system first. Then, we use the grating groove active control technology to rule an echelle grating of size 35 × 90 mm. In order to compensate the grating substrate surface error accurately, we exclude the surface error, which is caused by the testing mirror. The experiment results show that the ruled grating wavefront value is 0.056λ. Compared with the grating substrate surface error, which is 0.105λ at +36th order, the grating wavefront value has reduced by about 47%. In conclusion, the method can be used to compensate the grating surface error effectively and improve the grating wavefront quality significantly.

Funding

This work is supported by the National Natural Science Foundation of China (grant no. 61505204), the Chinese Finance Ministry for the National R&D Projects for Key Scientific Instruments (grant no. ZDY2008-1), the Ministry of National Science and Technology for National Key Basic Research Program of China (grant no. 2014CB049500), and the Key Science and Technology Program of Jilin province (grant no. 20180201030GX).

References

[1] Q.H. Yang, Compact high-resolution littrow conical diffraction spectrometer, Appl. Opt. 55 (18) (2016) 4801–4807.
[2] T. Jitsuno, S. Motokoshi, T. Okamoto, T. Mikami, D. Smith, M.L. Schattenburg, H. Kitamura, H. Matsuo, T. Kawasaki, K. Kondo, H. Shiraga, Y. Nakata, H. Habara, K. Tsubakimoto, R. Kodama, K.A. Tanaka, N. Miyanaga, K. Mima, Development of 91 cm size gratings and mirrors for LEFX laser system, J. Phys: Conf. Ser. 112 (3) (2008) 1–4.
[3] B. Gao, T. Chen, V. Khuat, J.h. Si, X. Hou, Fabrication of grating structures on silicon carbide by femtosecond laser irradiation and wet etching, Chin. Opt. Lett. 14 (2) (2016) 021407.
[4] S. Yokozeki, S. Sawa, Interferometric testing of grating using moire method, Japan. J. Appl. Phys. 14 (1) (1975) 465–470.
[5] Z. Jaroszewicz, Interferometric testing of the spacing error of a plane diffraction grating, Opt. Commun. 60 (6) (1986) 345–349.
[6] G.R. Harrison, The production of diffraction gratings I. development of the ruling art, J. Opt. Soc. Amer. 39 (6) (1949) 413–425.
[7] G.R. Harrison, G.W. Stroke, Interferometric control of grating ruling with continuous carriage advance, J. Opt. Soc. Amer. 45 (2) (1955) 112–120.
[8] G.R. Harrison, Techniques for Ruling Improved Large Diffraction Gratings Final Report, Massachusetts Institute of Technology, 1971, pp. 1–14.
[9] C. Yang, X.T. Li, H.L. Yu, J.W. Zhu, S.W. Zhang, J.X. Gao, Bayanheshig, Y.G. Tang, Practical method study on correcting yaw error of 500 mm grating blank carriage in real time, Appl. Opt. 54 (13) (2015) 4084–4088.
[10] C. Yang, H.L. Yu, J.C. Cui, X.T. Li, . Bayanheshig, X.D. Qi, Y.G. Tang, Real-time monitoring of ruling grating resolution by digital wavefront, Appl. Opt. 54 (3) (2015) 492–497.
[11] G.R. Harrison, S.W. Thompson, H. Kazukonis, J.R. Connell, 750-mm ruling engine producing large gratings and echelles, J. Opt. Soc. Amer. 62 (6) (1972) 751–756.
[12] T. Kita, T. Harada, Ruling engine using a piezoelectric device for large and high-groove density gratings, J. Opt. Soc. Amer. 31 (10) (1992) 1399–1406.
[13] H.L. Yu, X.T. Li, J.W. Zhu, H.Z. Yu, X.D. Qi, S.L. Feng, Reducing the line-curvature error of mechanically ruled gratings by interferometric control, Appl. Phys. 117 (1) (2014) 279–286.
[14] X.T. Li, Machine-Ruling Grating'S Line Error and Its Correction Method, (Ph.D. dissertation), University of Chinese Academy of Sciences, 2013.
[15] M.G. Moharam, T.K. Gaylord, Three-dimensional vector coupled-wave analysis of planar-grating diffraction, J. Opt. Soc. Amer. 73 (9) (1983) 1105–1112.
[16] Bayanheshig, The second kind angular dispersion and the analysis of characteristics of diffraction grating, Acta Phys. Sin. 53 (7) (2004) 2118–2122.
[17] S.Q. Zhu, H.X. Zou, X.C. Bao, H.L. Guo, Diffraction grating, 1987.
[18] C. Yang, H.L. Yu, X.T. Mi, Bayanheshig, Y.G. Tang, Development of the workbench yaw angle correction mechanism of large grating ruling machine, Chin. J. Sci. Instrum. 35 (15) (2014) 1065–1071.
[19] C. Yang, H.L. Yu, S.L. Feng, X.T. Li, X.D. Qi, S. Jang, Y.G. Tang, Influence of ruling accuracy of ruling carriage system on grating spectrum performance, Opt. Precision Eng. 22 (10) (2014) 2674–2682.